



Extended-synaptotagmin 1 engages in unconventional protein secretion mediated via SEC22B⁺ vesicle pathway in liver cancer

Kohji Yamada^{a,1,2}, Saya Motohashi^{a,1}, Tsunekazu Oikawa^b, Naoko Tago^a, Rei Koizumi^a, Masaya Ono^c, Toshiaki Tachibana^d, Ayano Yoshida^a, Saishu Yoshida^a, Masayuki Shimoda^e, Masahiro Oka^f, Yoshihiro Yoneda^{g,3}, and Kiyotsugu Yoshida^{a,2}

Edited by Ana Maria Cuervo, Albert Einstein College of Medicine, Bronx, NY; received February 14, 2022; accepted June 29, 2022

Protein secretion in cancer cells defines tumor survival and progression by orchestrating the microenvironment. Studies suggest the occurrence of active secretion of cytosolic proteins in liver cancer and their involvement in tumorigenesis. Here, we investigated the identification of extended-synaptotagmin 1 (E-Syt1), an endoplasmic reticulum (ER)-bound protein, as a key mediator for cytosolic protein secretion at the ER-plasma membrane (PM) contact sites. Cytosolic proteins interacted with E-Syt1 on the ER, and then localized spatially inside SEC22B⁺ vesicles of liver cancer cells. Consequently, SEC22B on the vesicle tethered to the PM via Q-SNAREs (SNAP23, SNX3, and SNX4) for their secretion. Furthermore, inhibiting the interaction of protein kinase C δ (PKC δ), a liver cancer-specific secretory cytosolic protein, with E-Syt1 by a PKC δ antibody, decreased in both PKC δ secretion and tumorigenicity. Results reveal the role of ER-PM contact sites in cytosolic protein secretion and provide a basis for ER-targeting therapy for liver cancer.

cytosolic protein secretion | PKC δ | endoplasmic reticulum (ER) | liver cancer | SEC22B

In eukaryotes, protein secretion is a fundamental mechanism for the communication between cells for developmental processes, maintenance of homeostasis, and tumor initiation and progression. Secretory proteins are translocated to the exterior of the cell through the process of membrane penetration. The general secretory proteins encode an N-terminal signal peptide that allows binding to the signal recognition particle for penetration into the endoplasmic reticulum (ER) through translocon pores (1), and are subsequently exported to the Golgi for extracellular secretion (2, 3). This process is often referred to as conventional secretion. Recently, many cases of cytosolic protein secretion have also been recognized independently on the conventional ER-Golgi secretion pathway, and these have been implicated in a variety of biological processes, including development, inflammation, and neurodegeneration (4–6). Unlike the unique route of conventional secretion, the secretion mechanism of cytosolic proteins has been categorized into two major routes: a direct path through the plasma membrane (PM) (e.g., fibroblast growth factor 2) (7) and another via vesicular trafficking (e.g., interleukin [IL]-1 β , and Acb 1) (8, 9), which is involved in various types of organelles, such as autophagosomes, lysosomes, and the ER-Golgi intermediate compartment (ERGIC) (10–12). Although these mechanisms of cytosolic protein secretion have almost been studied as inflammatory and neurogenerative events, it remains unclear whether comparable mechanisms extend to other diseases, including cancer.

The ER occupies the largest volume for any intracellular compartment, and synthesizes proteins that encode N-terminal signal peptides and lipids. The ER membrane is distributed throughout the cell and often forms contact sites in the vicinity of membranes of different organelles to regulate organelle dynamics and trigger organelle biogenesis, such as autophores and autophagosomes (13, 14). Autophagosome formation is considered to originate from membranes of the ER at ER-mitochondria or ER-PM contact sites (14, 15). Interestingly, autophagosomes are reported to be involved in the secretion of IL-1 β , a secretory protein that lacks an N-terminal signal peptide, in inflammatory cells (10, 11). Recent studies have shown that SEC22B, a member of the ER-bound tethering factors for ER-to-Golgi transport, is implicated in secretion of IL-1 β (10). SEC22B is also known to be accumulated at the ER-PM contact sites (16, 17). However, it remains unknown whether cytosolic protein secretion is involved in the ER or ER-PM contact sites.

Previous studies have reported several cytosolic proteins that are actively secreted from cancer cell lines, such as protein kinase C δ (PKC δ), importin α 1, nucleolin (NCL), and HSP90, and their involvement in tumor growth (18–22). In particular, extracellular PKC δ binds to cell surface glypican-3 and EGF receptors in liver cancer cells and activates growth signals, such as ERK1/2 (18, 19). The secretory events of

Significance

Autophagy is a process to degrade intracellular components for cellular survival, and implicated in many diseases, including cancer. Herein, we describe that the autophagy system engages in the secretion pathway of cytosolic proteins in liver cancer cells. We identify extended-synaptotagmin 1 (E-Syt1), an endoplasmic reticulum-bound protein localized at contact sites with the plasma membrane, as a key mediator to trigger cytosolic protein secretion. We observe that cytosolic proteins are enclosed in SEC22B⁺ vesicles in both cultured cells and tumor tissues of liver cancer, but not normal cells. Furthermore, targeting cytosolic proteins-to-E-Syt1 interaction by intracellular delivery of antibody suppresses tumorigenicity. These results provide a molecular mechanism on cancer-related unconventional protein secretion and a rational for an organelle-targeting therapy against liver cancer.

Author contributions: K. Yamada and S.M. designed research; K. Yamada, S.M., T.O., N.T., R.K., M. Ono, T.T., A.Y., and S.Y. performed research; M.S. contributed new reagents/analytic tools; K. Yamada, S.M., T.O., M. Ono, T.T., S.Y., M. Oka, Y.Y., and K. Yoshida analyzed data; and K. Yamada and K. Yoshida wrote the paper.

The authors declare no competing interest.

This article is a PNAS Direct Submission.

Copyright © 2022 the Author(s). Published by PNAS. This article is distributed under [Creative Commons Attribution-NonCommercial-NoDerivatives License 4.0 \(CC BY-NC-ND\)](https://creativecommons.org/licenses/by-nc-nd/4.0/).

¹K. Yamada and S.M. contributed equally to this work.

²To whom correspondence may be addressed. Email: kyamada@jikei.ac.jp or kyoshida@jikei.ac.jp.

³Present address: Research Institute for Microbial Diseases, Osaka University, Osaka 565-0871, Japan.

This article contains supporting information online at [http://www.pnas.org/lookup/suppl/doi:10.1073/pnas.2202730119/-/DCSupplemental](https://www.pnas.org/lookup/suppl/doi:10.1073/pnas.2202730119/-/DCSupplemental).

Published August 31, 2022.

some cytosolic proteins, such as PKC δ and HSP90, have been suggested to initiate from the cytosol; however, it is unclear as to which intracellular membranes are involved in cytosolic protein secretion.

Results

PKC δ Interacts with E-Syt1 at the ER in Liver Cancer Cells. We explored the interaction between intracellular membrane and secretory cytosolic proteins with a proximity biotinylation method using cultured liver cancer cells that constantly secrete cytosolic proteins under normal culture conditions (23). PKC δ was used as a model for secretory cytosolic proteins due to its high specificity for liver cancer (18). Liver cancer HepG2 clones stably expressing full-length PKC δ fused to proximity-dependent biotin identification 2 (BioID2), a modified promiscuous biotin ligase (24), were established to gain biotinylated proteins that interact with cytosolic PKC δ (*SI Appendix, Fig. S1 A–C*). We confirmed the similarity between PKC δ –BioID2 fusion and endogenous PKC δ based on the manner of secretion: that is, active secretion under physiological culture conditions and an inhibitory effect by treatment with phorbol 12-myristate 13-acetate (18) (*SI Appendix, Fig. S1A*).

Interactome analysis of affinity-purified biotinylated proteins in the membrane fraction (including the PM and organelles, except for the nucleus) revealed several ER-bound proteins, such as extended-synaptotagmin 1 (E-Syt1), chloride channel CLIC like 1 (CLCC1), starch binding domain 1, and stromal interaction molecule 1 (STIM1) as strong hits that were common to two PKC δ –BioID2-expressing clones (Fig. 1*A* and *SI Appendix, Table S1*). Among them, E-Syt1, which had the highest hit value, is known to be a tethering factor of ER–PM contact sites together with STIM1 (16). It is generally known that most E-Syt families, such as E-Syt2 and E-Syt3, are distributed along the PM, whereas only E-Syt1 has different localizations not only at the ER–PM contact sites, but also on the ER membrane in the cytoplasm (25–27). Therefore, this localization pattern of E-Syt1 might allow cytoplasmic proteins easily to access the ER. Indeed, the result of the interactome analysis was validated by a series of experiments, such as immunoblot of streptavidin-purified biotinylated proteins using PKC δ –BioID2-expressing HepG2 cells and colocalization studies of normal immunofluorescent observation, and proximity ligation assay (PLA) (Fig. 1*B–E* and *SI Appendix, Fig. S2A*).

To further examine the interaction of PKC δ with the ER, we performed a colocalization study using Sec61 β as an ER marker. Superresolution imaging with structured illumination microscopy (SIM) revealed that some PKC δ resides adjacent to the ER (Fig. 1*D*). Similar observations were obtained by PLA analysis (Fig. 1*F*), indicating that PKC δ interacts with the ER membrane. Importantly, this localization of PKC δ on the ER was significantly decreased when E-Syt1 was depleted (Fig. 1*F* and *SI Appendix, Fig. S2A*), indicating that PKC δ localization in the ER is dependent on E-Syt1. In addition, few colocalization of PKC δ with E-Syt1 or Sec61 β was observed in human normal hepatocytes and the gastric cancer cell line AGS, which lack the ability to secrete PKC δ (18) (Fig. 1*E* and *F* and *SI Appendix, Fig. S2B*). These results suggest that the E-Syt1–mediated localization of PKC δ in the ER is likely to contribute to PKC δ secretion.

E-Syt1 Is necessary for PKC δ Secretion in Liver Cancer Cells.

Next, we investigated the significance of E-Syt1 in PKC δ secretion by depleting E-Syt. Immunoblot analysis showed apparently

reduced levels of PKC δ in the media of E-Syt1 knockout (KO) cells (Fig. 2*A* and *SI Appendix, Fig. S3A*), indicating that E-Syt1 is required for PKC δ secretion. However, no effect on the secretion of α -fetoprotein (AFP), a classic secretory protein highly specific to liver cancer, was confirmed in the E-Syt1 KO cells (Fig. 2*A*), suggesting that the E-Syt1–mediated secretion pathway is different from conventional secretion. Similar results were obtained for importin α 1 secretion (Fig. 2*A*), strongly supporting the involvement of E-Syt1 in cytosolic protein secretion of liver cancer cells.

To further confirm PKC δ secretion, we established a cell-based assay using the HiBiT system to quantitate extracellular PKC δ (*SI Appendix, Fig. S1 D and E*). Decreased chemiluminescent signals were observed in E-Syt1 knockdown cells (Fig. 2*B* and *SI Appendix, Fig. S3 B–D*). Deletion mutant studies also demonstrated that weaker interactions with E-Syt1 were detected in cells expressing the C-terminal deletion mutant of PKC δ (Fig. 2*C* and *D*), indicating that C-terminal regions of PKC δ are necessary for its interaction with E-Syt1. We also confirmed an apparent decrease in both colocalization with the ER and detection in media of HepG2 cells expressing the C-terminal deletion mutant of PKC δ (Fig. 2*E* and *F* and *SI Appendix, Fig. S4*).

Previous reports have reported the involvement of extracellularly secreted cytosolic proteins, including PKC δ , in tumorigenesis (18, 19, 28). To confirm the relationship between PKC δ binding to E-Syt1 and tumorigenesis, PKC δ KO cells were reintroduced with the WT or the Δ 601–676 mutant of PKC δ . Xenograft mouse model analysis showed that lower tumorigenesis was noted in mice bearing Δ 601–676 mutant cells, compared to cells expressing WT cells (Fig. 2*G* and *H*), indicating that E-Syt1–mediated PKC δ secretion contributes to tumorigenesis. Based on these results, we concluded that the interaction of PKC δ with E-Syt1 on the ER may be a key process for PKC δ secretion.

Autophagy-Related Factors Are Involved in PKC δ Secretion.

We have previously shown enhancement of cytosolic protein secretion (e.g., PKC δ and importin α 1) under low-nutrient conditions in liver cancer cells (18, 20). It is also known that E-Syt1 acts as a tethering factor at the ER–PM contact sites, where autophagosomes are synthesized de novo. Therefore, we hypothesized that PKC δ secretion may be linked to autophagy. The level of PKC δ secretion was significantly enhanced when HepG2 cells were cultured under nutrient-starved Earle's balanced salt solution (EBSS) culture conditions (Fig. 3*A* and *SI Appendix, Fig. S5A*). We simultaneously confirmed that there was no PKC δ leakage by membrane disruption during the EBSS culture (Fig. 3*B*). Similarly, we confirmed that induction of autophagy in liver cancer cells by treatment with the mammalian target of rapamycin inhibitor, rapamycin, apparently enhances PKC δ secretion (29) (*SI Appendix, Fig. S5 B and C*). It is also accepted that autophagy occurs constantly in liver cancer cells under normal culture conditions (30) (*SI Appendix, Fig. S5A*). Thus, we performed inhibitory experiments by employing further autophagy-related inhibitors. PKC δ secretion level was significantly decreased in a dose-dependent manner when normally cultured HepG2 cells were treated with an autophagy inhibitor against early-phase (LY2109761) (30) (*SI Appendix, Fig. S5D*).

In contrast, other inhibitors against digestion phase (chloroquine [CQ] and bafilomycin A1 [BafA1]) showed no effect on PKC δ secretion (*SI Appendix, Fig. S5E*), suggesting that the mechanism of PKC δ secretion is mediated by common factors

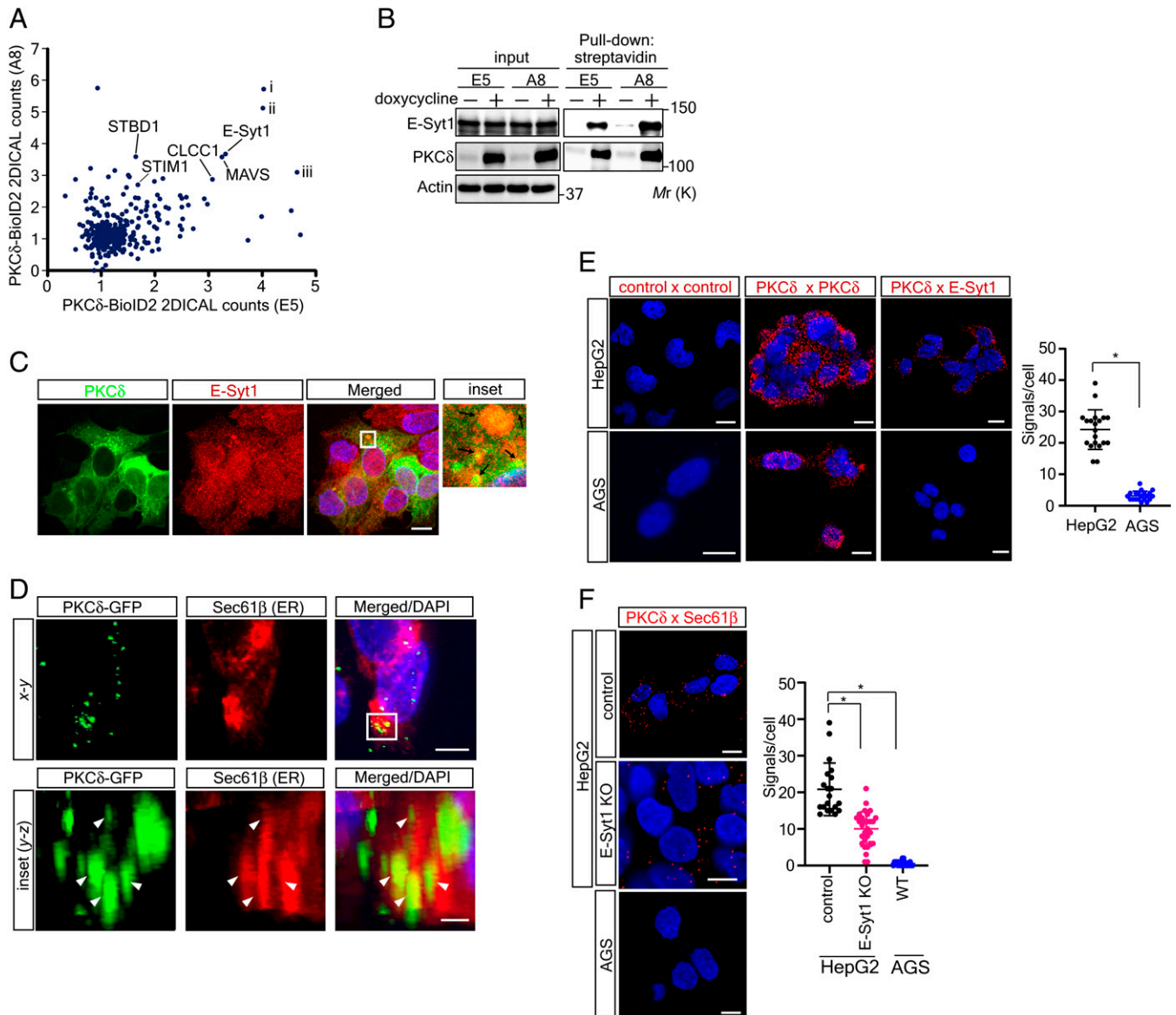


Fig. 1. BioID screen to identify putative membrane interactors with cytosolic PKC δ reveals E-Syt1. (A) The 2DICAL analysis of biotinylated proteins purified from the membrane fraction of two HepG2 cells stably expressing PKC δ -BioID2 (clone E5 or A8). The 360 counts of 2DICAL were calculated by comparing doxycycline-treated cells with untreated cells that do not express PKC δ -BioID2. Specificity is defined as having threefold more spectral counts in both E5 and A8 clones. The ER-bound proteins (e.g., E-Syt1 and CLCC1) and the mitochondrial intermembrane protein (mitochondrial antiviral-signaling protein) are identified. Other proteins found at comparable levels were abundant cytoplasmic or nuclear proteins (*i*, PRKAR2A; *ii*, TPD52L2; and *iii*, LBR). (B) Immunoblot analysis of biotinylated proteins purified with streptavidin from lysates in clone E5 or A8 cells; $n = 3$; independent experiments. Cells were treated with or without 1 μ g/mL doxycycline to induce PKC δ -BioID2 expression. Actin was used as the loading control. (C) Confocal micrographs to depict colocalization of endogenous PKC δ and E-Syt1 in HepG2 cells. Images are representative of three independent experiments. (Scale bars, 10 μ m.) (Inset) Magnified view of the region in the white box ($\times 5.5$). (D) Doxycycline-inducible PKC δ -GFP-expressing stable HepG2 cells were incubated with 0.5 μ g/mL doxycycline for 24 h, fixed, and stained with an antibody to Sec61 β as an ER marker. The stained cells were imaged with superresolution microscopy (3D SIM). Images from a single plane (x - y) and 3D reconstructed images (Inset: magnified view of the region in the white box, y - z) are shown. Arrowheads indicate the colocalization between PKC δ -GFP and the ER. Images are representative of three independent experiments. (Scale bars, 5 μ m.) (E) Confocal micrographs to detect the interaction with PKC δ and E-Syt1 in HepG2 and AGS cells. Each cell is fixed, reacted with combinations of mouse anti-PKC δ and rabbit anti-E-Syt1 antibodies (PKC δ \times E-Syt1), or mouse IgGs and rabbit IgGs (control \times control), or mouse anti-PKC δ antibody and rabbit anti-PKC δ antibody (PKC δ \times PKC δ), and subjected to Duolink in situ PLA. Data are shown as mean \pm SD ($n = 20$ for HepG2 cells and $n = 20$ for AGS cells), $*P < 0.0001$ (two-tailed Mann-Whitney test). Images are representative of three independent experiments. (Scale bars, 10 μ m.) (F) Confocal micrographs to detect the interaction with PKC δ and Sec61 β (an ER marker) in parental HepG2 (control), E-Syt1 KO HepG2 (E-Syt1 KO), or AGS cells. Each cell is fixed, reacted with a combination of mouse anti-PKC δ and rabbit anti-Sec61 β antibodies (PKC δ \times Sec61 β), and subjected to Duolink in situ PLA. Data are shown as mean \pm SD ($n = 20$ for control HepG2 cells and $n = 29$ for E-Syt1 KO HepG2 cells and $n = 20$ for AGS WT cells), $*P < 0.0001$ (two-tailed Mann-Whitney test). Images are representative of three independent experiments. (Scale bars, 10 μ m.)

of autophagy at a relatively early-stage, but at the late (or intermediate) stage, diverged from autophagy toward secretion. In accordance with this suggestion, PKC δ secretion was markedly diminished in knockdown cells of autophagy-induced factors (ATG5, ATG7, ATG16L1, p62, and LC3B) (Fig. 3 C and D and SI Appendix, Fig. S5 F–I). Colocalization of PKC δ with LC3B was also observed in HepG2 cells under both 10% fetal

bovine serum (FBS) (Fig. 3 E and F) and EBSS (Fig. 3 G and SI Appendix, Fig. S5 J) culture conditions. We also confirmed the colocalization of E-Syt1 with LC3B in EBSS-cultured cells (SI Appendix, Fig. S5 J). We further confirmed the specificity of PKC δ -LC3B localization using AGS cells (Fig. 3 H).

Accumulating evidence has demonstrated the involvement of autophagosomes in cytosolic protein secretion, also called

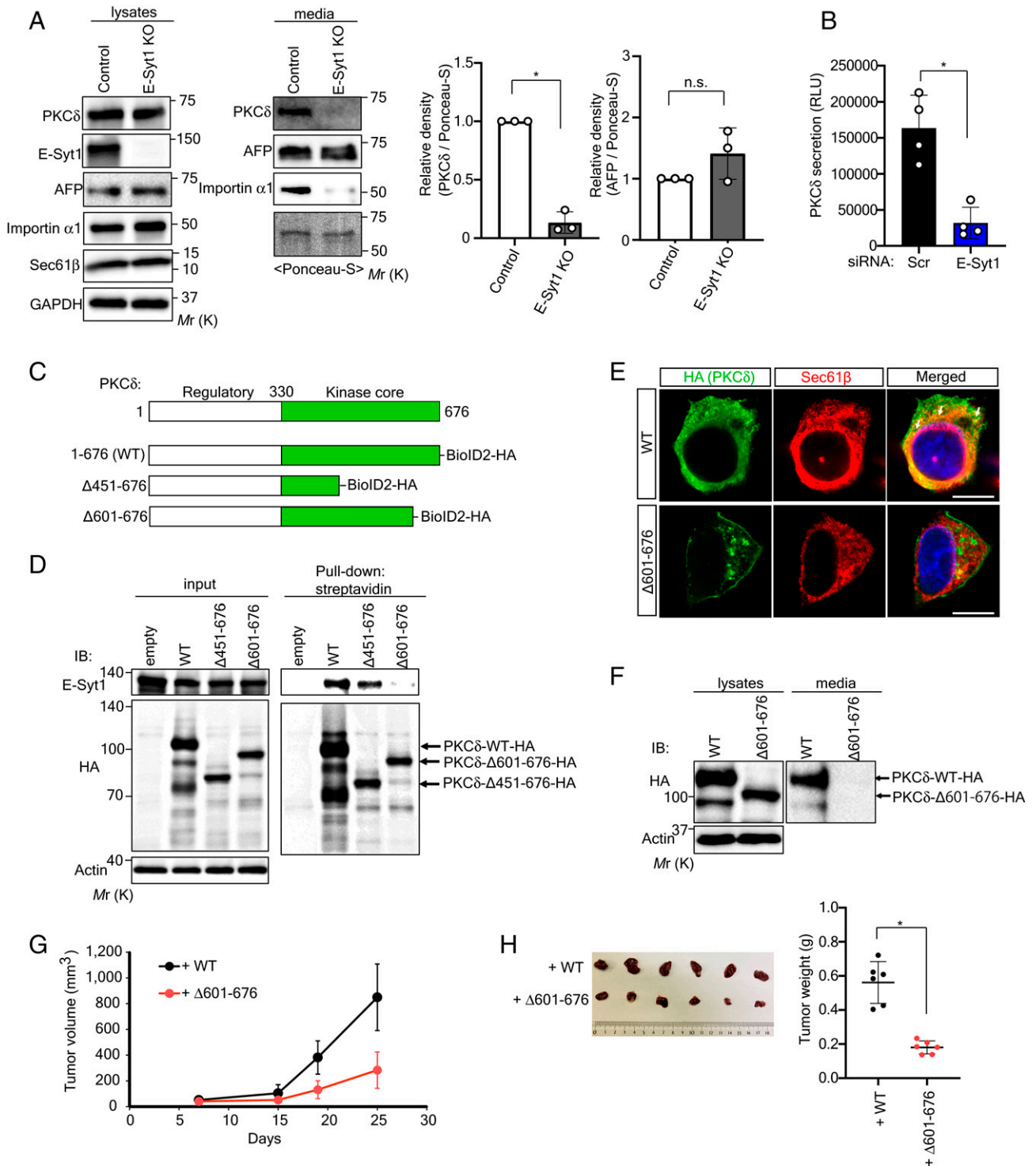


Fig. 2. E-Syt1 is necessary for PKC δ secretion. (A) Immunoblot analysis of lysates and media from control or E-Syt1 KO HepG2 cells showed that depletion of E-Syt1 reduces PKC δ level in media; $n = 3$; independent experiments. The relative signal density was quantified, and data are shown as mean \pm SD, $*P < 0.0001$ (two-tailed Student's t test); n.s., not significant. GAPDH and Ponceau-S stain were used as the loading control for lysates or media, respectively. (B) PKC δ secretion measured by HiBiT extracellular assay in doxycycline-inducible HepG2 cells treated with scrambled (Scr) or E-Syt1 siRNA for 24 h; $n = 4$ independent experiments. Luminescence was measured after cells were recultured with a medium containing 0.5 μ g/mL doxycycline for 24 h. Data are shown as mean \pm SD, $*P = 0.0053$ (Welch's t test). (C) Schematics of human PKC δ WT and deletion mutants (Δ 451-676 and Δ 601-676). These PKC δ constructs are fused with BiID2 and HA-epitope tag. (D) Immunoblot analysis of biotinylated proteins purified with streptavidin and lysates in doxycycline-inducible HepG2 cells transfected with empty or WT, Δ 451-676 or Δ 601-676 of PKC δ -BiID2-hemagglutinin (HA) vector to show a weak interaction with E-Syt1 when the C-terminal region of PKC δ is deleted; $n = 3$; independent experiments. Cells were treated with 1 μ g/mL doxycycline for 24 h. Representative blot is shown. Actin was used as the loading control. (E) Confocal micrographs of doxycycline-inducible HepG2 cells transfected with WT, or Δ 601-676 of PKC δ -BiID2-HA vector showing lack of colocalization between PKC δ and Sec61 β (an ER marker). Images are representative of two independent experiments. (Scale bar, 10 μ m.) (F) Immunoblot analysis of lysates and media in doxycycline-inducible HepG2 cells transfected with WT or Δ 601-676 of PKC δ -BiID2-HA vector to show less detection of Δ 601-676 of PKC δ in media; $n = 3$; independent experiments. Cells were treated with 1 μ g/mL doxycycline for 24 h. Actin was used as the loading control. (G) PKC δ KO HepG2 cells expressing PKC δ WT or Δ 601-676 were inoculated subcutaneously into nude mice ($n = 6$ per group). Tumor size was monitored. (H) Microscopic images and tumor weight of PKC δ KO HepG2 expressing PKC δ WT or Δ 601-676 ($n = 6$ per group) tumors. Error bars, mean \pm SD, $*P = 0.022$ (two-tailed Mann-Whitney test).

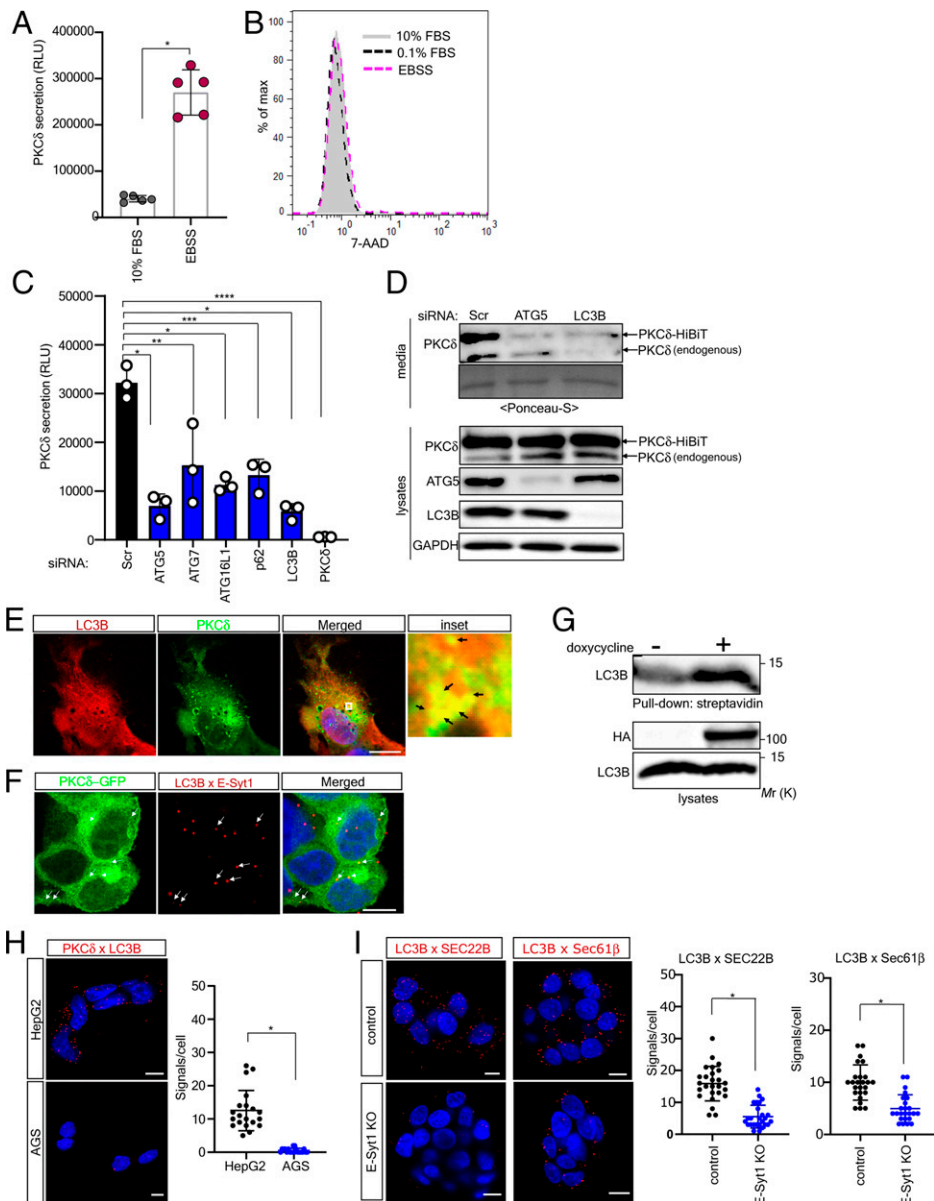


Fig. 3. Autophagy-related proteins are utilized for PKC δ secretion. (A) PKC δ secretion measured by HiBiT extracellular assay in doxycycline-inducible HepG2 cells preincubated with 0.5 μ g/mL doxycycline in 10% FBS-containing medium for 24 h, and stimulated with 10% FBS-containing medium or EBSS medium for 6 h; $n > 3$ independent experiments. Data are shown as mean \pm SD, $*P < 0.0001$ (two-tailed Student's t test). (B) Flow cytometric analysis of doxycycline-treated HepG2 cells incubated under 10% FBS-containing (black dashes), 0.1% FBS-containing (gray area), or EBSS (pink dashes) medium conditions for 6 h to show no leakage of PKC δ by disruption of the plasma membrane under each medium condition. Representative data are shown from three individual experiments. (C) PKC δ secretion measured by HiBiT extracellular assay in doxycycline-inducible HepG2 cells treated with scrambled (Scr), ATG5, ATG7, ATG16L1, p62, LC3, or PKC δ (as a positive control) siRNAs (2 nM) for 48 h; $n = 3$ independent experiments. Luminescence was measured after the cells were recultured with a medium containing 0.5 μ g/mL doxycycline for 24 h. Data are shown as mean \pm SD, $*P < 0.001$; $**P = 0.0292$; $***P = 0.0022$; $****P < 0.0001$ (ANOVA). (D) Immunoblot analysis of lysates and media from doxycycline-inducible HepG2 cells treated with scrambled (Scr), ATG5, or LC3 siRNAs (2 nM) for 48 h to show comparable inhibition of secretion on PKC δ -HiBiT fusion and endogenous PKC δ . Representative images are shown from three individual experiments. GAPDH and Ponceau-S stain were used as the loading control for lysates and media, respectively. (E) Confocal micrographs showing localization of endogenous PKC δ and LC3B in HepG2 cells cultured with 10% FBS-containing medium. Images are representative of three independent experiments. (Inset) Magnified view of the region in the white box ($\times 10$). Black arrows indicate colocalization between PKC δ and LC3B. (Scale bars, 10 μ m.) (F) Confocal micrographs to show the interaction with PKC δ -GFP, E-Syt1, and LC3B in doxycycline-inducible PKC δ -GFP-expressing HepG2 cells. Cells were treated with 1 μ g/mL doxycycline for 24 h, fixed, reacted with a combination of mouse anti-LC3B and rabbit anti-E-Syt1 antibodies (LC3B \times E-Syt1), and subjected to Duolink in situ PLA. White arrows indicate colocalization of PKC δ and PLA signals. Images are representative of two independent experiments. (Scale bars, 10 μ m.) (G) Immunoblot analysis of biotinylated proteins purified with streptavidin in clone E5 cells; $n = 3$; independent experiments. Cells were treated with or without 1 μ g/mL doxycycline. (H) Confocal micrographs to detect the interaction with PKC δ and LC3B (an autophagosome marker) in HepG2 or AGS cells. Each cell is fixed, reacted with a combination of mouse anti-PKC δ and rabbit anti-LC3B antibodies (PKC δ \times LC3B), and subjected to Duolink in situ PLA. Data are shown as mean \pm SD ($n = 20$ for HepG2 cells and $n = 20$ for AGS cells), $*P < 0.0001$ (two-tailed Mann-Whitney test). Images are representative of three independent experiments. (Scale bars, 10 μ m.) (I) Confocal micrographs to detect the interaction with LC3B and SEC22B or Sec61 β (an ER marker) in parental HepG2 (control), E-Syt1 KO HepG2 (E-Syt1 KO) cells. Each cell is fixed, reacted with a combination of mouse anti-LC3B and rabbit anti-SEC22B or Sec61 β antibodies (LC3B \times SEC22B or LC3B \times Sec61 β), and subjected to Duolink in situ PLA. Data are shown as mean \pm SD (LC3B \times SEC22B; $n = 26$ for control cells and $n = 26$ for E-Syt1 KO cells, LC3B \times Sec61 β ; $n = 25$ for control cells and $n = 24$ for E-Syt1 KO cells), $*P < 0.0001$ (two-tailed Mann-Whitney test). Images are representative of two independent experiments. (Scale bars, 10 μ m.)

secretory autophagy, in immune cells (10). In addition, these secretory autophagosomes are suggested to harbor SEC22B as an R-SNARE on their membrane surface instead of Stx17, which is necessary for promoting autophagosome–lysosome fusion and cargo degradation (31). Furthermore, it is generally accepted that SEC22B is a member of the ER–PM contact sites (17). Therefore, we examined relationship between SEC22B-mediated secretory autophagy and E-Syt1 in liver cancer cells. Levels of the interaction with LC3B and SEC22B was significantly reduced in E-Syt1 KO cells (Fig. 3*J*). We also revealed that the interaction with LC3B and Sec61 β depended on the expression of E-Syt1 (Fig. 3*J*). These results suggested that it is likely to be the accumulation of secretory autophagy-related factors on the ER is critical for PKC δ secretion.

Cytosolic Proteins Are Involved in SEC22B⁺ Vesicles for Their Secretion in Liver Cancer Cells. Next, we investigated whether SEC22B is involved in PKC δ secretion in liver cancer cells. PKC δ secretion was significantly decreased by depletion of SEC22B (Fig. 4 *A* and *B* and *SI Appendix*, Fig. S6 *A–C*), suggesting that SEC22B is essential for PKC δ secretion. Proximal interaction between PKC δ and SEC22B was also observed in the vicinity of the PM of HepG2 cells, but not in any cells that do not secrete PKC δ (e.g., E-Syt1 KO HepG2 cells and AGS cells) (Fig. 4*C*), indicating that the interaction between PKC δ and SEC22B is essential for PKC δ secretion.

It is often accepted that secretion of many cytosolic proteins, including IL-1 β , is mediated by relocalization of the Golgi reassembly stacking protein (GRASP), especially GRASP55 (32–34). Therefore, to investigate the effect of GRASP on PKC δ secretion, we carried out an RNA interference study of GRASP55. Interestingly, no effect on PKC δ secretion was seen in GRASP55 knockdown cells under 10% FBS culture condition, whereas EBSS stimulation slightly but significantly decreased in PKC δ secretion of GRASP55 knockdown cells (Fig. 4*D* and *SI Appendix*, Fig. S6*D*), indicating that GRASP55 is not necessarily required for PKC δ secretion in liver cancer cells. We also confirmed that PKC δ secretion is independent of TMED10 (*SI Appendix*, Fig. S6 *D* and *E*). Given that PKC δ is constantly secreted in liver cancer cells, these results suggest that the mechanism of PKC δ secretion may differ from that of typical secretory autophagy.

Given that a series of autophagy pathways are manifested as membrane trafficking, PKC δ secretion is also likely to be involved in vesicle transport. As expected, membrane-included PKC δ , in intracellular membranes, was detected by a biochemical protection assay using membrane fractions treated with protease K to digest membrane-bound surface proteins in HepG2 cells, but not in E-Syt1, ATG5, or SEC22B-depleted HepG2 cells (*SI Appendix*, Fig. S6 *F–H*). To further visualize positional information between PKC δ and SEC22B in the cytosol, we performed transmission electron microscopy (TEM). Enclosed PKC δ into SEC22B⁺ vesicles was frequently observed in HepG2 cells (Fig. 4 *E*, *Left*). SEC22B⁺ vesicles enclosing PKC δ were abundantly observed near the PM, which correlated with the results of PLA analysis (Fig. 4 *C* and *E*). In addition, the moment of fusion between a SEC22B⁺ vesicle and the PM, and of PKC δ secretion was observed by TEM (Fig. 4 *E*, *Right*), suggesting that SEC22B⁺ vesicle transport may be a key process in the fusion with the PM for secretion of cytosolic proteins in cancer cells. To confirm interactors with SEC22B⁺ vesicles at the PM, we performed an RNA interference study targeting Q-SNAREs of the PM (10, 35). A pronounced decrease in PKC δ secretion was noted when SNAP23, STX3, and STX4 (36) were knocked down in HepG2 cells (Fig. 4*F*

and *SI Appendix*, Fig. S6*I*). Furthermore, to examine the specificity of this secretory pathway in vivo, we employed human tumor tissues of hepatocellular carcinoma, and found that interactions between PKC δ and SEC22B were more observed in cells of tumor lesions than in nontumor lesions (Fig. 4*G* and *SI Appendix*, Fig. S6*J*).

To further examine the relationship between SEC22B⁺ vesicle-related PKC δ secretion and autophagy for protein degradation, HepG2 cells were treated with BafA1. As expected, BafA1 treatment did not affect the number of PKC δ –SEC22B interactions, although an increase in the number of Stx17–PKC δ interactions was observed in BafA1-treated cells (Fig. 4*H*). Taken together, these results suggest that SEC22B⁺ vesicles are critical organelles for PKC δ secretion in liver cancer cells.

To know whether the E-Syt1–SEC22B–SNAP23/STX3,4-secretory pathway is generalizable to other secreted cytosolic proteins in liver cancer cells, we examined secretion of importin α 1 and NCL. As a result, secretion of both importin α 1 and NCL depended on these factors (Fig. 5 *A–F* and *SI Appendix*, Fig. S7). These results indicate that the E-Syt1–SEC22B–SNAP23/STX3,4 pathway is a common mechanism of cytosolic protein secretion in liver cancer cells (Fig. 5*G*).

Inhibition of PKC δ –E-Syt1 Interaction Suppresses both PKC δ Secretion and Tumorigenesis. To examine the impact of mechanisms of cytosolic protein secretion on cancer, we performed intracellular delivery of PKC δ antibodies with DeliverIN transfection reagent as a drug delivery system. PKC δ secretion was markedly suppressed in HepG2 cells intracellularly derived with a PKC δ antibody recognizing its C terminus (C-20) that could block the PKC δ –ER interaction (Fig. 6 *A–C* and *SI Appendix*, Fig. S8 *A* and *B*), whereas no change in PKC δ secretion was observed in those cells using another PKC δ antibody that recognizes the N terminus (BD) (*SI Appendix*, Fig. S8*C*), which inhibits cell growth by targeting cell surface PKC δ (18). Our previous study has shown that treatment with C-20 antibody alone does not affect the growth of HepG2 cells (18). Intracellular delivery of C-20 antibody also resulted in a remarkable decrease in the proliferation of liver cancer cell lines (HepG2, Hep3B, and HuH7 cells) (Fig. 6 *D–F*), but not in AGS cells, which do not secrete PKC δ (Fig. 6*G*), suggesting that PKC δ secretion via E-Syt1 is responsible for liver cancer cell proliferation. To further evaluate the effect of PKC δ secretion on tumorigenesis, we carried out a three-dimensional (3D) spheroid formation assay (*SI Appendix*, Fig. S8*D*). C-20 antibody alone had no effect on HepG2 spheroid formation, whereas intracellular delivery of the C-20 antibody using DeliverIN significantly reduced the number and growth of HepG2 spheroids (Fig. 6 *H* and *I*). In contrast, no change of the number of spheroids by intracellular delivery of the C-20 antibody using DeliverIN was confirmed in AGS cells (*SI Appendix*, Fig. S8 *D–F*). These results suggest that targeting the interaction with E-Syt1 may be a useful therapeutic strategy for liver cancer.

Discussion

In this study, we describe a series of cancer-related unconventional protein secretion mechanisms in terms of: 1) interaction with E-Syt1 at the ER, 2) inclusion into SEC22B⁺ vesicles, and 3) fusion with the inner membrane of the PM. We also found that this secretion depends on autophagy-related proteins. This E-Syt1–SEC22B secretion system is highly specific for liver cancer cells and it is absent in cells that cannot secrete PKC δ . It is generally accepted that tumor tissues, especially in advanced cancers, frequently suffer from extracellular leakage of

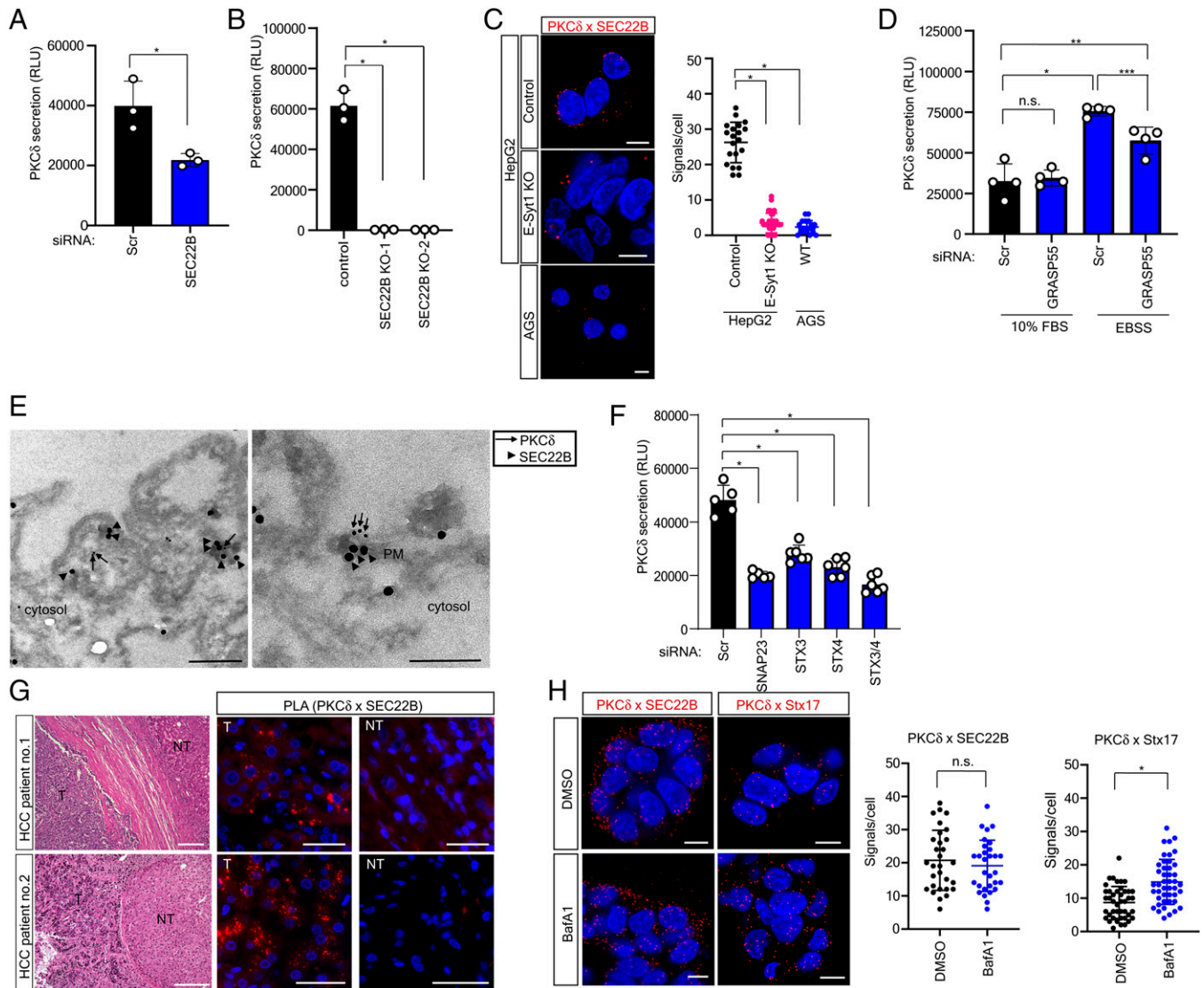


Fig. 4. PKC δ is secreted via SEC22B⁺ vesicle. (A) PKC δ secretion measured by HiBiT extracellular assay in doxycycline-inducible HepG2 cells treated with scrambled (Scr) or SEC22B siRNAs (2 nM) for 48 h; $n = 3$; independent experiments. Luminescence was measured after cells were recultured with a medium containing 0.5 $\mu\text{g}/\text{mL}$ doxycycline for 24 h. Data are shown as mean \pm SD, $*P = 0.0223$ (two-tailed Student's t test). (B) PKC δ secretion measured by HiBiT extracellular assay in doxycycline-inducible SEC22B KO HepG2 cells; $n = 3$; independent experiments. Luminescence was measured after cells were recultured with a medium containing 0.5 $\mu\text{g}/\text{mL}$ doxycycline for 24 h. Data are shown as mean \pm SD, $*P = 0.0002$ (two-tailed Student's t test). (C) Confocal micrographs to indicate the proximity with PKC δ and SEC22B in parental HepG2 (control), E-Syt1 KO HepG2 (E-Syt1 KO), or AGS cells. Each cell is fixed, reacted with a combination of mouse anti-PKC δ and rabbit anti-SEC22B antibodies (PKC δ \times SEC22B), and subjected to Duolink in situ PLA. Data are shown as mean \pm SD ($n = 20$ for control HepG2 cells and $n = 31$ for E-Syt1 KO HepG2 cells, and $n = 20$ for AGS WT cells), $*P < 0.0001$ (two-tailed Mann-Whitney test). Images are representative of three independent experiments. (Scale bars, 10 μm .) (D) PKC δ secretion measured by HiBiT extracellular assay in doxycycline-inducible HepG2 cells treated with scrambled (Scr) or GRASP55 siRNAs (2 nM) for 48 h; $n = 4$ independent experiments. Luminescence was measured after cells were recultured with normal 10% FBS-containing medium or EBSS with 0.5 $\mu\text{g}/\text{mL}$ doxycycline for 24 h. Data are shown as mean \pm SD, $*P = 0.0027$, $**P = 0.0112$, $***P = 0.0061$ (ANOVA), n.s., not significant. (E) Electron micrographs of HepG2 cells showing the existence of PKC δ (arrows) in SEC22B⁺ (arrowheads) vesicles at the vicinity of the PM (Left) and moment of the vesicle-PM fusion and secretion of PKC δ (Right). Images are representative and two similar independent experiments were performed. (Scale bars, 100 nm.) (F) PKC δ secretion measured by HiBiT extracellular assay in doxycycline-inducible HepG2 cells treated with scrambled (Scr), SNAP23, STX3, STX4, or a mixture with STX3 and STX4 siRNAs (2 nM) for 48 h; $n > 3$; independent experiments. Luminescence was measured after the cells were recultured with a medium containing 0.5 $\mu\text{g}/\text{mL}$ doxycycline for 24 h. Data are shown as mean \pm SD, $*P < 0.0001$ (ANOVA). (G) Images of tumor tissues of patients with hepatocellular carcinoma to indicate tumor cell-specific colocalization of PKC δ with SEC22B using Duolink in situ PLA (Center and Right). Tumor (T) and nontumor (NT) lesion were defined by evaluating H&E staining of each tumor section (Left). Two lines of images are representative in sections of five patients with liver cancer. (Scale bars, 50 μm .) (H) Confocal micrographs to detect the interaction with PKC δ and SEC22B or Stx17 in HepG2 cells treated with DMSO or BafA1 (100 nM) for 6 h. Each cell is fixed, reacted with a combination of mouse anti-PKC δ and rabbit anti-SEC22B or Stx17 antibodies (PKC δ \times SEC22B or PKC δ \times Stx17), and subjected to Duolink in situ PLA. Data are shown as mean \pm SD (PKC δ \times SEC22B; $n = 30$ for DMSO-treated and $n = 30$ for BafA1-treated cells, PKC δ \times Stx17; $n = 43$ for DMSO-treated and $n = 44$ for BafA1-treated cells), $*P < 0.0001$ (two-tailed Student's t test), n.s., not significant. Images are representative of two independent experiments. (Scale bars, 10 μm .)

cytosolic proteins mainly due to necrosis in tumors. However, many studies have already accumulated evidence on active cytosolic secretion in cultured cancer cells even under normal conditions, which is implicated in their involvement of tumorigenesis (18, 20, 28). Therefore, we assume that this cytosolic protein secretion mechanism provides a profound understanding of

cancer cell properties, especially in the early-stage cancer, and is a potential therapeutic target for patients. In fact, inhibition of cytosolic protein secretion by antibody delivery could suppress the tumorigenicity of liver cancer cells. The development of optimal modalities to target the E-Syt1-SEC22B pathway is an urgent issue for treatment of liver cancer.

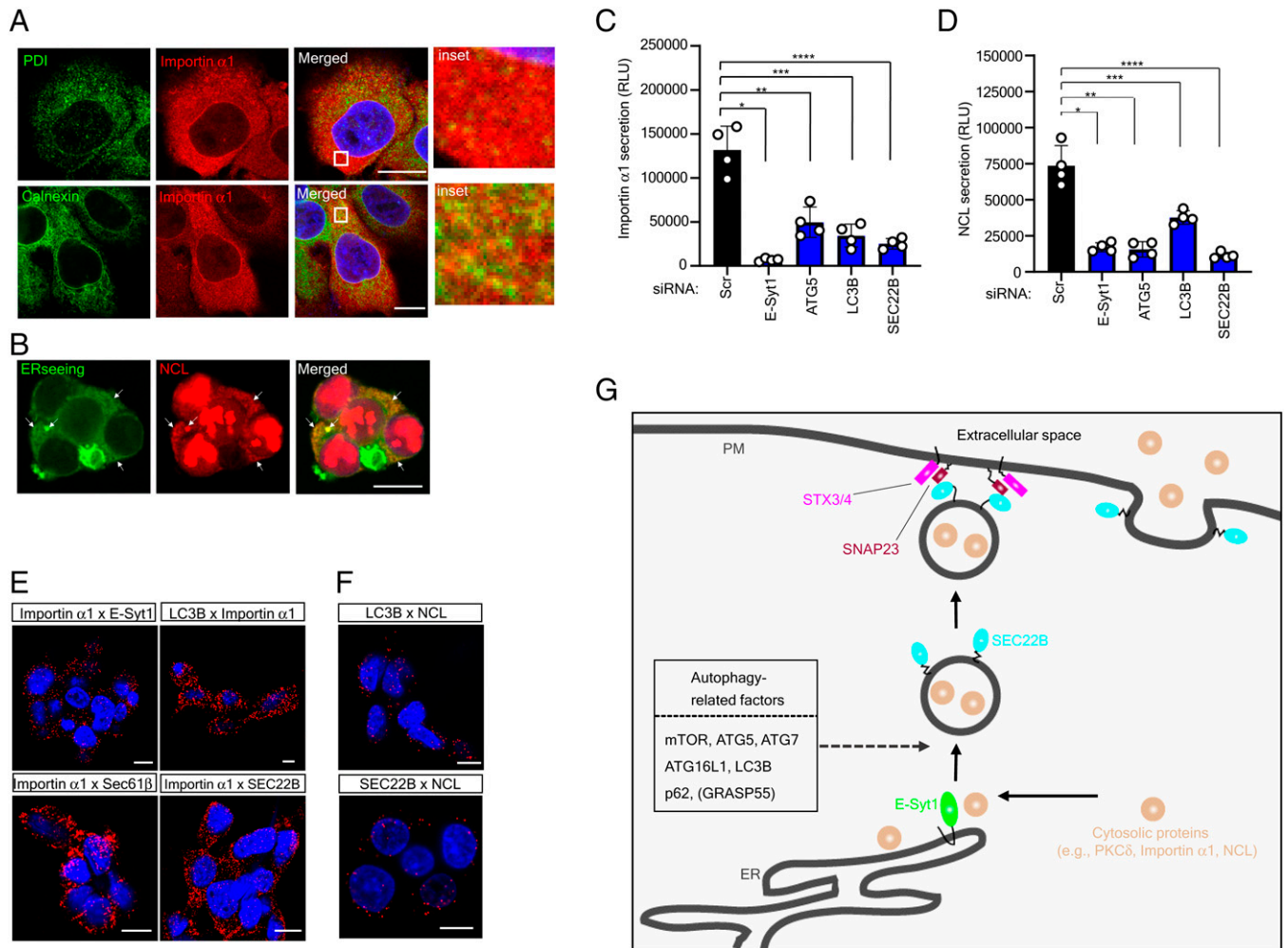


Fig. 5. Other cytoplasmic proteins are secreted via the same autophagy-related system. (A) Confocal micrographs showing colocalization of endogenous importin $\alpha 1$ with PDI or Calnexin in HepG2 cells. Images are representative of three independent experiments. (Scale bars, 10 μm .) (*Insets*) Magnified views of the regions in the white boxes, *Upper*: (x 10), *Lower*: (x 5). (B) Confocal micrographs showing colocalization of endogenous NCL with ER using ERseeing in HepG2 cells. Images are representative of three independent experiments. White arrows indicate colocalization of NCL with the ER. (Scale bar, 10 μm .) (C) Importin $\alpha 1$ secretion measured by HiBIT extracellular assay in doxycycline-inducible HepG2 cells treated with scrambled (Scr), E-Syt1, ATG5, LC3, or SEC22B siRNAs (2 nM) for 48 h; $n = 4$ independent experiments. Luminescence was measured after cells recultured with medium containing 1 $\mu\text{g}/\text{mL}$ doxycycline for 24 h. Data are shown as means \pm SD, $*P < 0.0002$; $**P = 0.0018$; $***P = 0.0104$; $****P = 0.0001$ (ANOVA). (D) NCL secretion measured by HiBIT extracellular assay in doxycycline-inducible HepG2 cells treated with scrambled (Scr), E-Syt1, ATG5, LC3, or SEC22B siRNAs (2 nM) for 48 h; $n = 4$ independent experiments. Luminescence was measured after cells recultured with medium containing 1 $\mu\text{g}/\text{mL}$ doxycycline for 24 h. Data are shown as means \pm SD, $*P < 0.001$; $**P = 0.0022$; $***P = 0.0007$; $****P = 0.0003$ (ANOVA). (E) Confocal micrographs to detect the interaction with importin $\alpha 1$ and indicated proteins in HepG2 cells. Cells are fixed, reacted with combination of mouse anti-importin $\alpha 1$ or LC3B and rabbit antibodies, and subjected to Duolink in situ PLA. The images are representative of two independent experiments. (Scale bars, 10 μm .) (F) Confocal micrographs to detect the interaction with NCL and LC3B or SEC22B in HepG2 cells. Cells are fixed, reacted with combination of mouse anti-LC3B or SEC22B and a rabbit anti-NCL antibody, and subjected to Duolink in situ PLA. The images are representative of two independent experiments. (Scale bars, 10 μm .) (G) A model for the role of E-Syt1 as a link between the ER and vesicle-mediated secretion of cytosolic proteins. Packaging of cytosolic proteins into SEC22B⁺ vesicles is apparently dependent on the expression of E-Syt1 and autophagy-related proteins. E-Syt1 may form a specific complex for cytosolic protein secretion at the ER in liver cancer cells.

The importance in this study is that cytosolic protein secretion in cancer cells has both similarities and differences compared to previously reported cytosolic protein secretion. The main similarity is the involvement of autophagy factors. It has been reported that autophagy factors (e.g., ATG5, ATG7, ATG16L1, p62, and LC3B) are implicated in the secretion of IL-1 β . Similarly, in this study, we found that cytosolic protein secretion in liver cancer cells is autophagy factors-dependent. In contrast, there is an important difference with respect to the manner of secretion induction. Although secretion of many reported cytosolic proteins is generally triggered by specific stimuli, such as inflammation, the secretion of PKC δ , importin $\alpha 1$, and NCL in liver cancer cells occurs even under normal culture conditions. In particular, PKC δ is known to be detected at higher levels in the blood of patients with hepatocellular

carcinoma than in patients with chronic liver disease (18). Therefore, we speculate that cytosolic protein secretion in liver cancer cells may be an essential property that cells need to acquire as cancer cells. Furthermore, we found that this cytosolic protein secretion under normal culture conditions was independent of GRASP55, a common feature of secretion of many cytosolic proteins, such as IL-1 β . Hence, we predict that cytosolic protein secretion in liver cancer cells may have a potentially distinctive mechanism that is still undefined.

In this study, our findings indicate that cytosolic protein secretion initiates from the ER, although limited to liver cancer. Previous studies on the origin of cytosolic protein secretion have shown the relocalization of GRASP55, which is often known to be involved in the stacking of Golgi cisternae and the tethering of vesicles destined to fuse with the Golgi apparatus

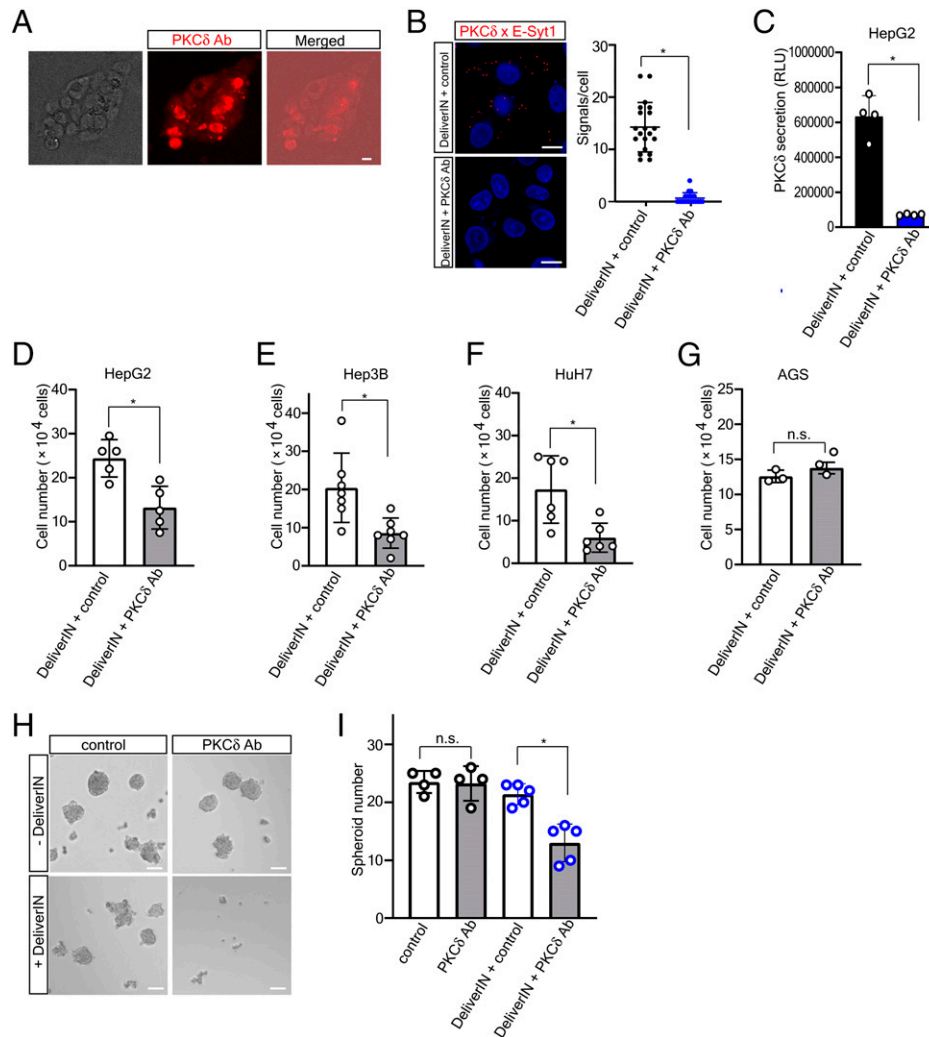


Fig. 6. Targeting interaction between PKC δ and E-Syt1 inhibits liver cancer cell growth. (A) Images of intracellular delivery of PKC δ antibody (Ab) (C-20) using Ab-DeliverIN transfection reagent (DeliverIN; as a drug delivery system) in HepG2 cells. The epitope of the C-20 Ab on PKC δ is a C-terminal sequence of PKC δ , which was required for binding to E-Syt1 and the secretion (Fig. 2 D and F and *SI Appendix*, Fig. S8A). No intracellular accumulation of the Ab in HepG2 cells treated with only C-20 Ab is confirmed in *SI Appendix*, Fig. S8B. (Scale bars, 10 μ m.) (B) Confocal micrographs of HepG2 cells treated with DeliverIN and control IgGs or C-20 Ab showing the inhibition of the interaction with PKC δ and E-Syt1 in intracellular delivery of the C-20 Ab. Each cell is fixed, reacted with a combination of mouse anti-PKC δ and rabbit anti-E-Syt1 antibodies (PKC δ \times E-Syt1), and subjected to Duolink in situ PLA. Data are shown as mean \pm SD ($n = 20$ for the group of treatment with DeliverIN and control IgG, $n = 20$ for the group of treatment with DeliverIN and the C-20 Ab), $*P < 0.0001$ (two-tailed Student's t test). Images are representative of three independent experiments. (Scale bars, 10 μ m.) (C) PKC δ secretion measured by HiBIT extracellular assay in doxycycline-inducible HepG2 cells treated with DeliverIN and control IgGs or C-20 Ab for 24 h to show the suppression of PKC δ secretion by the intracellular delivery of the C-20 Ab; $n = 4$; independent experiments. 0.5 μ g/mL doxycycline was simultaneously added when DeliverIN and antibodies were treated. Data are shown as mean \pm SD, $*P < 0.0001$ (two-tailed Student's t test). (D–G) Proliferation assay by cell count of the indicated cell lines treated with control or C-20 Ab in the presence of DeliverIN for 48 h showing that the cell proliferative reduction by treatment with DeliverIN and the C-20 Ab specifically occurs in cell lines that secrete PKC δ . Haemocytometer was used for cell counting after trypan-blue staining to exclude dead cells, and each plot was an average of four fields of view. Similar experiments were independently repeated more than three times. Data are shown as mean \pm SD (D) $*P = 0.0047$ (Welch's t test); (E) $*P = 0.0129$ (Welch's t test); (F) $*P = 0.0153$ (Welch's t test); (G) n.s., not significant. (H) Images of HepG2 3D multicellular spheroid treated with control IgGs or C-20 Ab in the presence/absence of DeliverIN to show the anti-tumorigenic effect of the C-20 Ab with DeliverIN. (Scale bars, 20 μ m.) (I) The number of HepG2 3D multicellular spheroids was counted based on the criterion of size $> 25 \mu$ m. Three independent experiments were performed. Data are shown as mean \pm SD, $*P = 0.002$ (ANOVA); n.s., not significant.

(37), to the cytosolic protein secretion route, and the involvement of TMED10 as a transporter in the ERGIC (34). These previous findings have indirectly but implicated the Golgi, whereas our results demonstrated the impact of the ER localization, mainly supported by the evidence that the ER localization is regulated by E-Syt1. Indeed, the E-Syt1-related cytosolic protein secretion in liver cancer in the present study showed little involvement of GRASP55 or TMED10. Based on these results, we speculate that the cytosolic protein secretion in cancer cells is regulated by the ER and diverges into a secretory transport pathway. In support of this notion, other groups have shown that autophagy factors, such as ATG5, is observed at the

ER (15, 38). However, it is still unclear whether the ER is involved in the difference between autophagy and cytosolic protein secretory pathways, and why autophagy factors are involved in cytosolic protein secretion. These are the important questions to be addressed in future studies.

It is well known that E-Syt1 and SEC22B are essential members of ER-PM contact sites (25, 39). In fact, both the PKC δ -SEC22B interaction and PKC δ -containing SEC22B $^+$ vesicles were observed in the vicinity of the PM. Nevertheless, the majority of interactions of PKC δ with E-Syt1 or LC3B were observed at a considerable distance from the PM, and this discrepancy may be due to the fact that E-Syt1 is diffused

throughout the intracellular ER membrane (25). Taking these data together, we speculate that E-Syt1 may play a role in the recruitment of cytosolic PKC δ to the ER–PM contact sites.

Although our present study demonstrated the secretion mechanism by which cytosolic proteins are routed through the ER, we could not determine the mechanism by which these cytosolic proteins are enclosed in the membrane. One possible mechanism is that they are surrounded by autophagosomes at the ER or ER–PM contact sites. However, we consider this possibility to be unlikely because of observations for the monolayer membrane of SEC22B⁺ vesicles. In addition, PKC δ secretion was not affected by BafA1 treatment for inhibition of protein degradation, suggesting that the membrane trafficking route is different from that of autophagy for degradation. A possible scenario is that a double-bilayer organelle like autophagosomes is not utilized during the formation of autophagy factor-mediated vesicles for the cytosolic protein secretion, or there may be an unknown mechanism by which double-bilayer autophagosomes subject to membrane remodeling become monolayer membranes. As another possible mechanism, secreted cytosolic proteins such as PKC δ and importin α 1 may directly enter the ER. In this context, a recent report showed that IL-1 β penetrates the ERGIC via TMED10 (11). Analogous to this mechanism, it might also penetrate the ER via unidentified transporters at the ER–PM contact sites. For example, the nuclear localization signal, which is commonly involved in PKC δ , importin α 1, and NCL (40, 41), may be employed to penetrate the ER for cytosolic protein secretion.

In conclusion, we demonstrated that cytosolic protein secretion is initiated from the ER in liver cancer cells. Together with the fact that conventional secretion utilizes the ER, the ER is strongly proven to be an organelle specific to protein secretion regardless of the N-terminal signal peptide. Our study also suggests that this unconventional secretory system may be one of the processes that underlies cancer survivability, and thereby provides the rationale for exploring biomarkers and novel therapeutic strategies for liver cancer.

Materials and Methods

Cell Culture. Human liver cancer lines (HepG2, Hep3B, and HuH7) and human gastric cancer line AGS were obtained from the Japanese Collection of Research Bioresources in 2017. HepG2 Tet-On Advanced cells were purchased from Takara in 2018. Primary human hepatocytes were purchased from Lonza in 2021. HepG2 cells were maintained in Dulbecco's Modified Eagle's Medium (DMEM; Sigma) supplemented with 10% FBS (Sigma). AGS cells were maintained in RPMI1640 (Sigma) supplemented with 10% FBS. HepG2 Tet-On Advanced cells were maintained in α -MEM (Nacalai) supplemented with 0.1 mM NEAA, 500 μ g/mL G418, and 10% Tet system-approved FBS (Takara). Hepatocytes were maintained in HBM basal Medium (Lonza) supplemented with SignalQuots Kit (Lonza). For starvation, each cell was washed and cultured in EBSS (Sigma) for indicated times. Cell lines were routinely monitored for *Mycoplasma* (4A Biotech). The cell used for experiments were passaged within 10 times after thawing.

Pull-Down of Biotinylated Proteins. Biotinylated proteins by Biold2 were isolated, according to the conventional Biold protocol. Briefly, TRE-inducible HepG2 cells containing Biold2 constructs were grown in two 100-cm² dishes of biotin (50 μ M) and 1 μ g/mL doxycycline for 24 h before cell lysis. Cells were washed with PBS, collected using cell scraper, and resuspended in 1 mL lysis buffer (50 mM Tris-HCl [pH 7.6], 150 mM NaCl, 1 mM PMSF, 1 mM DTT, 10 μ g/mL aprotinin, 1 μ g/mL leupeptin, 1 μ g/mL pepstatin A, and 1% Nonidet P-40). After centrifugation at 20,000 \times g for 15 min, the supernatants were used as cell lysate for the following manipulation. The protein concentrations of the cell lysate were determined using the bicinchoninic acid (BCA) protein assay

(ThermoFisher). The cell lysate was incubated at 4 °C overnight with Dynabeads MyOne streptavidin C1 beads (ThermoFisher) that had been prewashed twice in the same buffer. The beads were washed with twice wash buffer 1 (2% SDS), three times in wash buffer 2 (1% Triton X-100, 0.1% deoxycholate, 500 mM NaCl, 1 mM EDTA, 50 mM Hepes, pH 7.5), and three times in wash buffer 3 (50 mM Tris pH 7.4, 50 mM). For mass spectrometry, the beads were incubated in 2% sodium deoxycholate. For immunoblotting, the beads were incubated with sodium dodecylsulfate (SDS) sampling buffer and boiled at 100 °C for 10 min.

Mass Spectrometry. To identify isolated proteins, a two-dimensional (2D) image-converted analysis of liquid chromatography and mass spectrometry (2DICAL) shotgun proteomics analysis was performed, as described previously (42, 43).

Small-Interfering RNA Knockdown. Knockdown experiments were performed using On-TARGETplus small-interfering RNA (siRNA) SMARTpool (Dharmacon GE) for E-Syt-1 (L-010652-00), PKC δ (L-003524-00), ATG5 (L-004374-00), ATG7 (L-020112-00), ATG16L1 (L-021033-01), p62/SQSTM1 (L-010230-00), LC3B (L-012846-00), SEC22B (L-011963-00), SNAP23 (L-017545-00), STX3 (L-015401-00), STX4 (L-016256-00), GRASP55 (L-019045-00), and TMED10 (L-003718-00). The cells were transfected using Lipofectamine RNAiMAX (ThermoFisher).

Cell-Based HiBiT Assay. Extracellular localized HiBiT-fused proteins were evaluated using a Nano-Glo HiBiT Extracellular Detection System (Promega), according to the manufacturer's instructions. Briefly, Tet-On HepG2 cells were plated into 96-well plate and treated with doxycycline for indicated times. Nano-Glo HiBiT Extracellular Detection reagents were added to all wells and the luminescence was measured after 5 min incubation by an Infinite 200PRO plate reader (Tecan).

Duolink In Situ PLA. Cells were fixed with 4% paraformaldehyde for 15 min, and permeabilized with 0.1% Triton X-100 for 5 min. After blocking, cells were then incubated with mouse following antibodies to: following antibodies to: PKC δ (BD Bioscience 610398; 1:500), LC3B (MBL 4E12; 1:1,000), SEC22B (Santacruz sc101267; 1:500), importin α 1 (BD Bioscience 610485; 1:200); and rabbit following antibodies: PKC δ (Santacruz sc937; 1:200), E-Syt1 (ATLAS HPA016858; 1:200), Sec61 β (CST #14648; 1:200), SEC22B (Abcam ab181076; 1:200), Stx17 (Abcam ab229646; 1: 200). The fluorescence signals were detected by the Duolink in situ PLA probe according to the manufacturer's instructions and visualized using a Zeiss LSM 880 laser microscope. The signals were quantified and processed using the ImageJ software (NIH).

Immunoelectron Microscopic Analysis. Cells were fixed in 4% paraformaldehyde in 0.1 M phosphate buffer (PB) for 2 h at room temperature. Dehydration was carried out using a graded series of ethanol. The cells were embedded in LR-White (Oken). Samples were incubated with primary antibodies against PKC δ (BD Bioscience 610398; 1:500) (18) and SEC22B (Abcam ab181076; 1:200), and labeled with secondary anti-mouse IgG (H+L) antibodies conjugated with 10-nm immunogold (BBI Solutions) or anti-rabbit IgG (H+L) antibodies conjugated with 20-nm immunogold (BBI Solutions). For TEM analysis, about 70-nm-thick sections were cut with a diamond knife, stained with uranyl acetate and lead citrate solutions, and observed with a JEOL JEM1400 Plus electron microscope at 100 Kv.

Clinical Samples. Tumor specimens from hepatocellular carcinoma patients were obtained at the Jikei University Hospital. The protocol used in the study conformed to the ethical guidelines of the 1975 Declaration of Helsinki and were approved by the Jikei University School of Medicine Ethics Review Committee [Ethics Approval License: 29-038 (8654) and 29-006 (8622)], and written informed consent was obtained from all patients.

Statistical Analysis and Reproducibility. Data are represented as mean \pm SD from the indicated number of replicates. Statistical analysis was performed by using the unpaired, two-tailed student's or Welch's *t* test, ANOVA, or Mann-Whitney tests using Prism 8 software (Graphpad), with *n* and *P* values states in the figure legends.

Extended materials and methods are provided in *SI Appendix*.

Data, Materials, and Software Availability. The unprocessed source data and the statistical source data that support the findings of this study are available from Mendeley Data (DOI: [10.17632/t2d9tm594w.1](https://doi.org/10.17632/t2d9tm594w.1), <https://data.mendeley.com/datasets/t2d9tm594w/1>) (44). Correspondence and requests for materials should be addressed to kyamada@jikei.ac.jp or kyoshida@jikei.ac.jp.

ACKNOWLEDGMENTS. We thank K. Aoki (The Jikei University) and M. Ohmura (Keio University) for valuable comments; K. Katagiri for experimental contributions; K. Sakurai for contributions to histological experiment; and K. Neishi for contributions to the superresolution data analysis. This work was supported by Grants from: the Japan Agency for Medical Research and Development Grants A440TR, B326TS, and JP21ck0106712 (to K. Yamada); the Japan Society for the Promotion of Science KAKENHI Grants JP16K18434, JP18K15253, and

JP20K07621 (to K. Yamada.), and JP17H03584, JP18K19484, and JP20H03519 (to K. Yoshida.); the Takeda Science Foundation (K. Yamada); and The Science Research Promotion Fund (K. Yoshida).

Author affiliations: ^aDepartment of Biochemistry, Jikei University School of Medicine, Tokyo 105-8461, Japan; ^bDivision of Gastroenterology and Hepatology, Department of Internal Medicine, Jikei University School of Medicine, Tokyo 105-8461, Japan; ^cDepartment of Clinical Proteomics, National Cancer Center Research Institute, Tokyo 104-0045, Japan; ^dCore Research Facilities for Basic Science, Research Center for Medical Sciences, Jikei University School of Medicine, Tokyo 105-8461, Japan; ^eDepartment of Pathology, Jikei University School of Medicine, Tokyo 105-8461, Japan; ^fLaboratory of Nuclear Transport Dynamics, National Institutes of Biomedical Innovation, Health and Nutrition, Osaka 567-0085, Japan; and ^gNational Institutes of Biomedical Innovation, Health and Nutrition, Osaka 567-0085, Japan

1. S. O. Shan, P. Walter, Co-translational protein targeting by the signal recognition particle. *FEBS Lett.* **579**, 921–926 (2005).
2. G. Zanetti, K. B. Pahuja, S. Studer, S. Shim, R. Schekman, COPII and the regulation of protein sorting in mammals. *Nat. Cell Biol.* **14**, 20–28 (2011).
3. A. Pantazopoulou, B. S. Glick, A kinetic view of membrane traffic pathways can transcend the classical view of Golgi compartments. *Front. Cell Dev. Biol.* **7**, 153 (2019).
4. J. P. Steringer, H. M. Müller, W. Nickel, Unconventional secretion of fibroblast growth factor 2–A novel type of protein translocation across membranes? *J. Mol. Biol.* **427**, 1202–1210 (2015).
5. C. Andrei *et al.*, The secretory route of the leaderless protein interleukin 1beta involves exocytosis of endolysosome-related vesicles. *Mol. Biol. Cell* **10**, 1463–1475 (1999).
6. P. Ejlerskov *et al.*, Tubulin polymerization-promoting protein (TPPP/p25 α) promotes unconventional secretion of α -synuclein through exophagy by impairing autophagosomelysosome fusion. *J. Biol. Chem.* **288**, 17313–17335 (2013).
7. T. Schäfer *et al.*, Unconventional secretion of fibroblast growth factor 2 is mediated by direct translocation across the plasma membrane of mammalian cells. *J. Biol. Chem.* **279**, 6244–6251 (2004).
8. M. Zhang, S. J. Kenny, L. Ge, K. Xu, R. Schekman, Translocation of interleukin-1 β into a vesicle intermediate in autophagy-mediated secretion. *eLife* **4**, e11205 (2015).
9. J. M. Duran, C. Anjard, C. Stefan, W. F. Loomis, V. Malhotra, Unconventional secretion of Acb1 is mediated by autophagosomes. *J. Cell Biol.* **188**, 527–536 (2010).
10. T. Kimura *et al.*, Dedicated SNAREs and specialized TRIM cargo receptors mediate secretory autophagy. *EMBO J.* **36**, 42–60 (2017).
11. M. Zhang *et al.*, A translocation pathway for vesicle-mediated unconventional protein secretion. *Cell* **181**, 637–652.e15 (2020).
12. C. Rabouille, Pathways of unconventional protein secretion. *Trends Cell Biol.* **27**, 230–240 (2017).
13. A. G. Manford, C. J. Stefan, H. L. Yuan, J. A. Macgurn, S. D. Emr, ER-to-plasma membrane tethering proteins regulate cell signaling and ER morphology. *Dev. Cell* **23**, 1129–1140 (2012).
14. A. C. Nascimbeni *et al.*, ER-plasma membrane contact sites contribute to autophagosome biogenesis by regulation of local PI3P synthesis. *EMBO J.* **36**, 2018–2033 (2017).
15. M. Hamasaki *et al.*, Autophagosomes form at ER-mitochondria contact sites. *Nature* **495**, 389–393 (2013).
16. B. Hewlett, N. P. Singh, C. Vannier, T. Galli, ER-PM contact sites–SNARING actors in emerging functions. *Front. Cell Dev. Biol.* **9**, 635518 (2021).
17. A. Gallo *et al.*, Role of the Sec22b-E-syt complex in neurite growth and ramification. *J. Cell Sci.* **133**, jcs247148 (2020).
18. K. Yamada *et al.*, Unconventional secretion of PKC δ exerts tumorigenic function via stimulation of ERK1/2 signaling in liver cancer. *Cancer Res.* **81**, 414–425 (2021).
19. K. Yamada *et al.*, Extracellular PKC δ signals to EGF receptor for tumor proliferation in liver cancer cells. *Cancer Sci.* **113**, 2378–2385 (2022).
20. K. Yamada *et al.*, Cell surface localization of importin α 1/KPNA2 affects cancer cell proliferation by regulating FGF1 signalling. *Sci. Rep.* **6**, 21410 (2016).
21. W. Qiu *et al.*, The involvement of cell surface nucleolin in the initiation of CCR6 signaling in human hepatocellular carcinoma. *Med. Oncol.* **32**, 75 (2015).
22. X. Wang *et al.*, The regulatory mechanism of Hsp90 α secretion and its function in tumor malignancy. *Proc. Natl. Acad. Sci. U.S.A.* **106**, 21288–21293 (2009).
23. K. J. Roux, D. I. Kim, M. Raida, B. Burke, A promiscuous biotin ligase fusion protein identifies proximal and interacting proteins in mammalian cells. *J. Cell Biol.* **196**, 801–810 (2012).
24. D. I. Kim *et al.*, An improved smaller biotin ligase for BioID proximity labeling. *Mol. Biol. Cell* **27**, 1188–1196 (2016).
25. S. W. Min, W. P. Chang, T. C. Südhof, E-Syts, a family of membranous Ca²⁺-sensor proteins with multiple C2 domains. *Proc. Natl. Acad. Sci. U.S.A.* **104**, 3823–3828 (2007).
26. F. Giordano *et al.*, PI(4,5)P(2)-dependent and Ca(2+)-regulated ER-PM interactions mediated by the extended synaptotagmins. *Cell* **153**, 1494–1509 (2013).
27. O. Idevall-Hagren, A. Lü, B. Xie, P. De Camilli, Triggered Ca²⁺ influx is required for extended synaptotagmin 1-induced ER-plasma membrane tethering. *EMBO J.* **34**, 2291–2305 (2015).
28. J. F. Wise *et al.*, Nucleolin inhibits Fas ligand binding and suppresses Fas-mediated apoptosis in vivo via a surface nucleolin-Fas complex. *Blood* **121**, 4729–4739 (2013).
29. P. Hu *et al.*, Autophagy suppresses proliferation of HepG2 cells via inhibiting glypican-3/wnt/ β -catenin signaling. *Oncotargets Ther.* **11**, 193–200 (2018).
30. K. Kiyono *et al.*, Autophagy is activated by TGF-beta and potentiates TGF-beta-mediated growth inhibition in human hepatocellular carcinoma cells. *Cancer Res.* **69**, 8844–8852 (2009).
31. J. New, S. M. Thomas, Autophagy-dependent secretion: mechanism, factors secreted, and disease implications. *Autophagy* **15**, 1682–1693 (2019).
32. M. A. Kinseth *et al.*, The Golgi-associated protein GRASP is required for unconventional protein secretion during development. *Cell* **130**, 524–534 (2007).
33. M. Chiritoiu, N. Brouwers, G. Turacchio, M. Pirozzi, V. Malhotra, GRASP55 and UPR control interleukin-1 β aggregation and secretion. *Dev. Cell* **49**, 145–155.e4 (2019).
34. J. Nüchel *et al.*, An mTORC1-GRASP55 signaling axis controls unconventional secretion to reshape the extracellular proteome upon stress. *Mol. Cell* **81**, 3275–3293.e12 (2021).
35. Y. A. Chen, R. H. Scheller, SNARE-mediated membrane fusion. *Nat. Rev. Mol. Cell Biol.* **2**, 98–106 (2001).
36. T. Wang, L. Li, W. Hong, SNARE proteins in membrane trafficking. *Traffic* **18**, 767–775 (2017).
37. J. Shorter *et al.*, GRASP55, a second mammalian GRASP protein involved in the stacking of Golgi cisternae in a cell-free system. *EMBO J.* **18**, 4949–4960 (1999).
38. E. Itakura, N. Mizushima, Characterization of autophagosome formation site by a hierarchical analysis of mammalian Atg proteins. *Autophagy* **6**, 764–776 (2010).
39. M. Petkovic *et al.*, The SNARE Sec22b has a non-fusogenic function in plasma membrane expansion. *Nat. Cell Biol.* **16**, 434–444 (2014).
40. T. S. Adwan, A. M. Ohm, D. N. M. Jones, M. J. Humphries, M. E. Reyland, Regulated binding of importin- α to protein kinase C δ in response to apoptotic signals facilitates nuclear import. *J. Biol. Chem.* **286**, 35716–35724 (2011).
41. Y. Yoneda, Nucleocytoplasmic protein traffic and its significance to cell function. *Genes Cells* **5**, 777–787 (2000).
42. M. Ono *et al.*, Biomarker discovery of pancreatic and gastrointestinal cancer by 2DICAL: 2-dimensional image-converted analysis of liquid chromatography and mass spectrometry. *Int. J. Proteomics* **2012**, 897412 (2012).
43. Y. Kagami *et al.*, Mps1 phosphorylation of condensin II controls chromosome condensation at the onset of mitosis. *J. Cell Biol.* **205**, 781–790 (2014).
44. J. Yamada, Data for “Extended-synaptotagmin 1 engages in unconventional protein secretion mediated via SEC22B+ vesicle pathway in liver cancer.” Mendeley Data. <https://data.mendeley.com/datasets/t2d9tm594w/1>. Deposited 19 August 2022.